

**CLASSIFICATION OF TUMOR FROM MRI IMAGES USING GABOR PATTERN**

**G.THAMARAI SELVI\***  
**K.DURAIAMY\*\***

\*Research Scholar, Anna University of Technology, Coimbatore, Tamil Nadu, India  
\*\*Dean (Academic), K.S.Rangasamy College of Technology, Tiruchengode, Tamil Nadu, India

---

**ABSTRACT**

Recognizing automatically the medical images is very tedious in the field of medical image processing. Medical images acquired from different modalities such as Computed Tomography (CT), Magnetic Resonance Imaging (MRI), functional Positron Emission Tomography (fPET), Ultrasonography, etc are used for the diagnosis purpose. The main complex problem in the medical field is the classification of the brain tumor images. The misclassification of MRI images such as normal or abnormal images occurs due to the human interpretation. In our research work, we extract the brain tumor from the MRI images using the Non - Local Gabor XOR pattern (NLGXP). The extracted feature is applied to a Feed Forward Neural Network (FFNN) which gives high accuracy.

**KEYWORDS:** MRI, Tumor, Classification, NLGXP, FFNN.

**1. INTRODUCTION**

Brain is the essential part of the human body and also the structure of the brain is very intricate. It is the complex organ and it is a part of the central nervous system (CNS). The brain is covered by a protective skull and consists of gray matter (GM), white matter (WM) and cerebrospinal fluid (CSF). This skull hides the brain from direct view, provides protection from injuries as well as hinders the study of its function in both health and diseases (Martini F.H, ed, 2004). However, brain can be affected by various diseases, which cause changes in its normal structure and behaviour. One major disease that severely affects the brain is brain tumor. Brain tumor is one of the major causes for the increase in Mortality among children and adults. A tumor is a mass of tissue that grows out of control of the normal forces that regulates growth. Brain tumor is a group of anomalous cells that grows inside or around the brain (Sebe et al, 2000). The occurrence of brain tumors is increasing hastily, mainly in the older population than the younger population. Tumors can directly devastate all the healthy brain cells.

## **2. RELATED WORK**

The existing work used Kohonen Neural Networks for image classification. Some modifications of the conventional Kohonen neural network are implemented which proved to be much superior to the conventional neural network (Messen et al., 2006). Forward back – propagation artificial neural network (FP – ANN) and K – nearest neighbor (K – NN) are used for the classification of MR brain images. The classification accuracy, sensitivity and specificity rate are high for K – NN. The disadvantage of this approach is that it requires fresh training each time whenever there is an increase in image database. But, this method required less computation time due to the feature reduction based (EL-Sayed and EL-Dahshan 2009).

Particle Swarm Optimization (PSO) based Counter Propagation Neural Network (CPN) classifier, are used for classification, where PSO is used as the optimization algorithm and it is used along with modified Counter Propagation Neural Network classifier. Conventional CPN modified CPN, PSO based CPN are analyzed in terms of classification accuracy and convergence time period. The results showed that PSO based modified CPN classifier have high performance measures (Jude Hemanth and Kezi Selva 2010).

A classification technique called Vector Seeded Region Growing (VSRG). Here, the pixel vectors have been selected by VSRG through standard deviation and relative Euclidean distance. With the aid of VSRG processing, the data dimensionality of MRI can be minimized and the desired target of interest can be achieved. The performance of the technique has been evaluated by conducting a series of experiments and compared with the commonly used C – means techniques. The result has shown the efficacy of this technique for MR image classification (Chuin-Mu Wang and Ruey-Maw Chen 2011). Pruned association rule with MARI algorithm based classifier was used for brain tumor classification. This approach is compared with Bayesian classifier and associative classifier. The result shows that the proposed method achieves high sensitivity, accuracy and less execution time (Rajendran and Madheswaran 2009).

## **3. PROPOSED METHOD**

In our proposed method, the following steps are followed:

- ❖ Preprocessing using Gaussian filter
- ❖ Feature extraction using Non-Local Gabor XOR Pattern
- ❖ Classification using the Feed Forward Network

### 3.1 PRE-PROCESSING

Brain images usually contain one or more type of noise and artifact. The input image is subjected to a set of pre-processing steps so that the image gets transformed to be suitable for the further processing. Here, preprocessing is to increase the contrast between normal and abnormal brain tissues. Here the Gaussian filter is used to reduce the noise and get a better image and improves the quality of the image.

#### 3.1.1 Gaussian Filter

A Gaussian filter is a filter whose impulse response is a Gaussian function. Gaussian filters are designed to shun the overshoot of step function input while diminishing the rise and fall time because the Gaussian filter has less possible group delay.

In mathematical terms, a Gaussian filter changes the input signal by convolution with a Gaussian function and so, this conversion is also called as Weierstrass transform.

$$F_c = \frac{F_s}{\sigma} \quad (1)$$

The 1D Gaussian filter is represented as,

$$g(x) = \frac{1}{\sqrt{2\pi}\sigma} e^{-\frac{x^2}{2\sigma^2}} \quad (2)$$

The impulse response of the 1D Gaussian Filter is,

$$g(x) = \frac{1}{\sqrt{2\pi}\sigma} e^{-\frac{\sigma^2 u^2}{2}} \quad (3)$$

### 3.1 EXTRACTION OF FEATURES USING NON-LOCAL GABOR XOR PATTERNS

Feature extraction plays an important role in tumor image identification and verification. The purpose of feature extraction is to reduce the original data set by measuring certain properties, or features, that distinguish one input pattern from another pattern. In our proposed work, we are slightly modifying the Local Gabor XOR pattern and it is used for feature extraction process and we have named it as Non-Local Gabor XOR Patterns. In our work, feature extraction is performed by following steps. Initially, input image is segmented into multiple blocks and each block is divided into 3 x 3 matrix form. Euclidean distance is determined between each block as follows.

Let  $P_i, P_j$  are the two pixels and  $i, j = 1, 2, \dots, MN$  where  $P_i$  is the first pixel of first block,  $P_j$  is the first pixel of second block. The pixel distance, written as  $|P_i - P_j|$  is the distance

between  $P_i$  and  $P_j$  of two blocks. For example, if  $P_i$  is at location  $(k,l)$  and  $P_j$  is at  $(k',l')$ ,  $|P_i - P_j|$  may be  $\sqrt{(k-k')(l+l')^2}$ . The Euclidean distance of two blocks  $P_i, P_j$  is written by

$$d_E^2(P_i, P_j) = \sqrt{\sum_{i,j=1}^{MN} (P_i - P_j)^2} \quad (4)$$

After ED process, LGXP is applied on this image in order to obtain the feature block.

LGXP Descriptor phases are quantized into different ranges. The number of phase ranges is made such a way that to make the patterns robust to the variations of Gabor phase (Shufu Xie et al 2010), hence cannot be too high. After the quantization process each of the phase value is quantized into the quantized level values.

$$q(\varphi_{\mu,w}(l)) = i \quad (5)$$

$$\text{if } \frac{360 * i}{c} \leq \varphi_{\mu,w}(l) < \frac{360 * (i+1)}{c}, i = 0, 1, \dots, c-1.$$

$\varphi_{\mu,w}(l)$  is the phase value of the pixel and  $q(\varphi_{\mu,w}(l))$  is the quantized value of the phase and  $c$  is the number of phase ranges.

The phase ranges is considered as 4 and are given the table below.

Phase Range (in degrees)	Quantized Phase Value
<b>0-89</b>	0
<b>90-179</b>	1
<b>180-269</b>	2
<b>270-359</b>	3

**Table 3.1** Quantized phase value for the input phase

We have opted for four phase range levels which achieve a good balance between the robustness to phase variations and representation power of local patterns. Subsequently LGXP operator is applied to the quantized phases of the central pixel and each of its neighbours.  $LGXP_{\mu,w}^i$  ( $P = 1, 2, \dots, P$ ) denotes the pattern calculated between  $\varphi_{\mu,w}(l)$  and its neighbor  $z_c$ , which is computed as follows:

$$LGXP_{\mu,w}^i = q(\varphi_{\mu,w}(z_c)) \text{ XOR } q(\varphi_{\mu,w}(z_i)) \quad (6)$$

where  $\varphi_{\mu,w}(z_c)$  denotes the phase and  $q(\varphi_{\mu,w}(z_i))$  is the quantized value of the phase and where  $\varphi_{\mu,w}(l)$  denotes the central pixel position in the Gabor phase map with scale  $w$  and orientation  $\mu$ ,  $p$  is the size of neighborhood XOR operation is defined as follows:

$$A \text{ XOR } B = \begin{cases} 0, & A = B \\ 1, & \text{otherwise} \end{cases} \quad (7)$$

Finally the resulting binary labels are concatenated together as the local pattern of the central pixel.  $LGXP_{\mu,w}(z_c) = \sum_{i=1}^p 2^{i-1} \cdot NLGXP_{\mu,w}^i$  After LGXP process, we get one equivalent value and this value is replaced for the original value and this process is repeated for every blocks. After feature extraction process, the features are extracted from the regions and those features are given to the Feed Forward Neural Network (Mishra 2010) for training.

### 3.1 Feed Forward Network

A layered feed-forward network consists of a certain number of layers, and each layer contains a certain number of units. There is an input layer, an output layer, and one or more hidden layers between the input and the output layer. Each unit receives its inputs directly from the previous layer (except for input units) and sends its output directly to units in the next layer (except for output units). Unlike the Recurrent network, which contains feedback information, there are no connections from any of the units to the inputs of the previous layers nor to other units in the same layer, nor to units more than one layer ahead. Every unit only acts as an input to the immediate next layer. Obviously, this class of networks is easier to analyze theoretically than other general topologies because their outputs can be represented with explicit functions of the inputs and the weights.

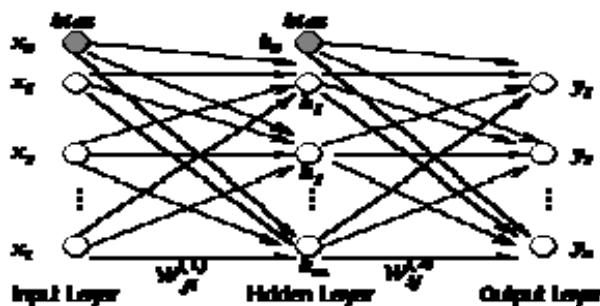


Figure 3.1 Feed-forward neural network

An example of a layered network with one hidden layer is shown in Figure 3.1. In this network there are  $l$  inputs,  $m$  hidden units, and  $n$  output units. The output of the  $j$ th hidden unit is obtained by first forming a weighted linear combination of the  $l$  input values, then adding a bias,

$$a_j = \sum_{i=1}^l w_{ji}^{(1)} x_i + w_{j0}^{(1)} \quad (8)$$

where  $w_{ji}^{(1)}$  is the weight from input  $i$  to hidden unit  $j$  in the first layer and  $w_{j0}^{(1)}$  is the bias for hidden unit  $j$ . If we are considering the bias term as being weights from an extra input (8) can be rewritten to the form of,

$$a_j = \sum_{i=1}^l w_{ji}^{(1)} x_i \quad (9)$$

The activation of hidden unit  $j$  then can be obtained by transforming the linear sum using an activation function  $g(x)$

$$h_j = g(a_j) \quad (10)$$

The outputs of the network can be obtained by transforming the activation of the hidden units using a second layer of processing units. For each output unit  $k$ , first we get the linear combination of the output of the hidden units,

$$a_k = \sum_{j=1}^m w_{kj}^{(2)} h_j + w_{k0}^{(2)} \quad (11)$$

Again we can absorb the bias and rewrite the above equation to,

$$a_k = \sum_{j=1}^m w_{kj}^{(2)} h_j \quad (12)$$

Then applying the activation function  $g_2(k)$  to (11) we can get the  $k$ th output

$$y_k = g_2(a_k) \quad (13)$$

Combining (9), (10), (12) and (13) we get the complete representation of the network as

$$y_k = g_2 \left( \sum_{j=0}^m w_{kj}^{(2)} g \left( \sum_{i=0}^l w_{ji}^{(1)} x_i \right) \right) \quad (14)$$

The network of Figure 3.1 is a network with one hidden layer. We can extend it to have two or more hidden layers easily as long as we make the above transformation further.

One thing we need to note is that the input units are very special units. They are hypothetical units that produce outputs equal to their supposed inputs. No processing is done by these input units.

#### 4. EXPERIMENTAL RESULTS AND DISCUSSION

This section describes the experimental results of our proposed Segmentation technique using brain MRI images with and without tumors. Our proposed approach is implemented in Matlab environment on Core 2 Duo, processor speed 1.6 GHz (mat lab

version 7.10). Here, we have tested our proposed tumor detection technique using medical images taken from the publicly available sources.

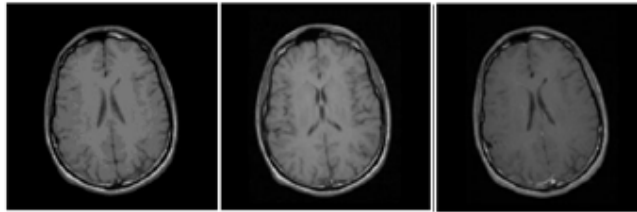


Fig.4.1 MRI image dataset without tumor MRI images

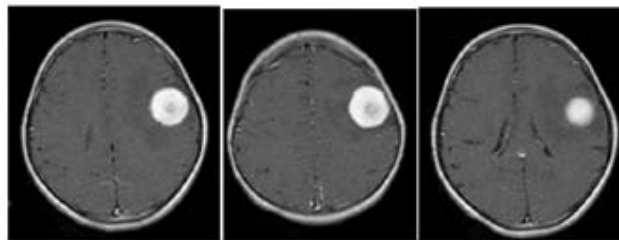
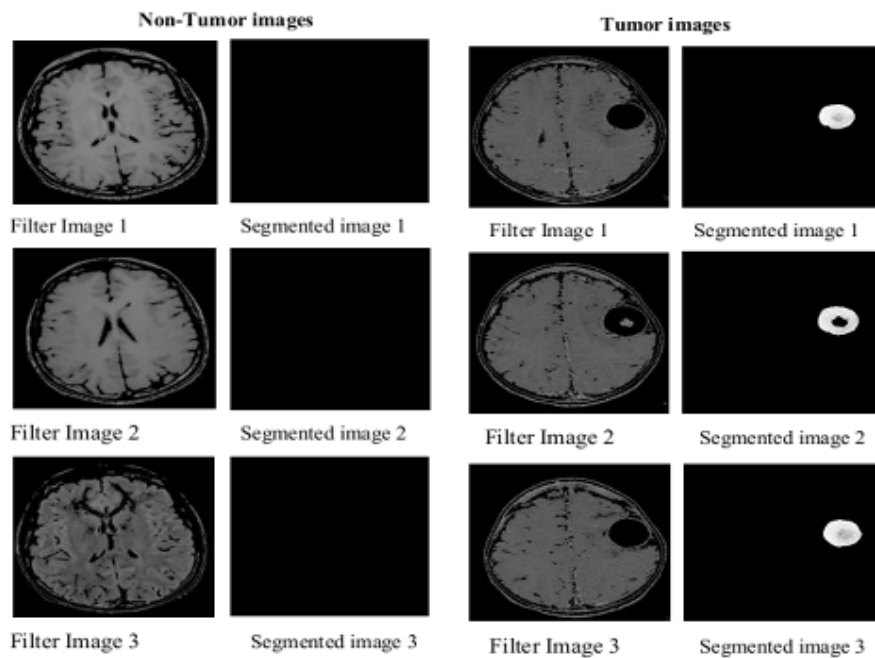


Fig.4.2 MRI image dataset with tumor MRI images



(a)

(b)

Fig.4.3 Experimental results, (a) MRI image without tumor and corresponding Segmented MRI image b) MRI image with tumor and corresponding Segmented MRI image

**4.1. Experimental results**

**4.1.1 PERFORMANCE ANALYSIS USING EVALUATION METRICS**

For a given disease condition, the most favourable test can be selected based on these attributes. Sensitivity, specificity, and accuracy are the extensively utilized statistics to define a diagnostic test. Especially, they are used to measure how superior and reliable a test is. As well, the how the image segmentation process could be found out in terms of quality rate.

In testing phase, the testing dataset is given to the FFNN technique (Quart-UI-Ain et al 2009) to find the tumors in brain images and the obtained results are evaluated through evaluation metrics namely, sensitivity, specificity and accuracy (Sasikala & Kumaravel 2008). In order to find these metrics, we first compute some of the terms like, True positive, True negative, False negative and False positive based on the definitions given in table 4.1.

<b>Experimental Outcome</b>	<b>Condition as determined by the Standard of Truth</b>		<b>Row Total</b>
	<i>Positive</i>	<i>Negative</i>	
<i>Positive</i>	TP	FP	TP+FP
<i>Negative</i>	FN	TN	FN + TN
Column total	TP+FN	FP+TN	N = TP+TN+FP+FN

Table 4.1 Table defining the terms TP, FP, FN, TN

The evaluation of brain tumor detection in different images is carried out using the following metrics (Wen Zhu et al, 2010) as suggested by the equations,

- ❖ **Sensitivity:** Sensitivity is a measure which determines the probability of the results that are true positive such that person has the tumor.

$$Sensitivity = TP / (TP + FN) \tag{15}$$

- ❖ **Specificity:** Specificity is a measure which determines the probability of the results that are true negative such that person does not have the tumor.

$$Specificity = TN / (TN + FP) \tag{16}$$

- ❖ **Accuracy:** Accuracy is a measure which determines the probability that how much results are accurately classified.



$$Accuracy = (TN + TP)/(TN + TP + FN + FP) \quad (17)$$

where, *TP* stands for True Positive, *TN* stands for True Negative, *FN* stands for False Negative and *FP* stands for False Positive.

Thus the outcomes of the experimentation proved with 90% of accuracy in tumor detection from brain MRI images using FFNN.

Evaluation metrics		Our Proposed Approach	
		Training dataset	Testing dataset
Input MRI image dataset	True Negative(TN)	4	5
	False Positive(FP)	1	0
	True Positive(TP)	5	3
	False Negative (FN)	0	2
	Specificity	0.8	1
	Sensitivity	1	0.6
	Accuracy	0.9	0.8

The evaluation graphs of the sensitivity, specificity and the accuracy graph are shown in figure 4.4 for the classification of tumor using FFNN. The graph is drawn between the Training and Testing Dataset.

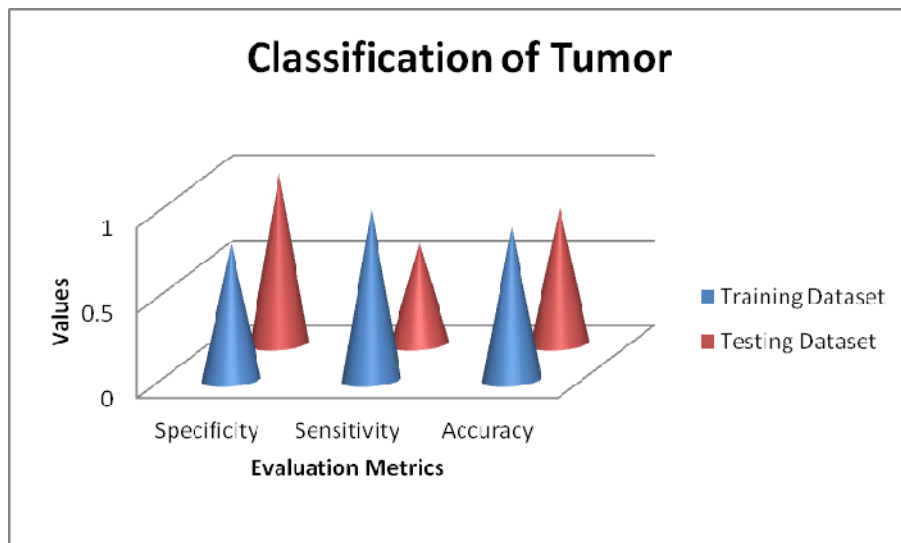


**Fig. 4.4 Graph of classification of tumor**

## **CONCLUSION**

Tumor image segmentation and extraction are an important and challenging factor in the medical image processing. In this paper, we have presented an effective tumor extraction approach from brain MRI images using NLGXP and the tumor classification is done by using FFNN. By using the techniques of NLGXP and FFNN, we have achieved high efficiency. The results for the tumor detection are validated through evaluation metrics namely, sensitivity, specificity and accuracy. This can be further extended to calculation the location and the size of the tumor region.

## **REFERENCES**

1. Chuin-Mu Wang & Ruey-Maw Chen 2011, 'Vector Seeded Region Growing for Parenchyma Classification in Brain MRI', *International Journal of Advancements in Computing Technology*, vol.3, no.2, pp. 1 – 11.
2. EL-Sayed, A & EL-Dahshan 2009, 'A hybrid technique for automatic MRI brain image Classification', *Studia Univ.Informatica*, vol. LIV, no. 1, pp. 109 – 115.
3. Jude Hemanth, D & Kezi Selva, C 2010, 'Performance Improved PSO based Modified Counter Propagation Neural for Abnormal MR Brain Image Classification', *International Journal of Advanced Soft Computing and Applications*, vol. 2, no. 1, pp. 1- 20.
4. Martin-Landrove , M & Villalta, R 2006, 'Brain tumor image segmentation using neural networks', *Proceedings of International Society of Magnetic Resonance in Medicine*, pp. 14:16.
5. Messen, Wehrens, R & Buydens, L 2006, 'Supervised Kohonen networks for classification problems', *Chemometrics and Intelligent Laboratory Systems* , vol. 8, no. 3, pp. 99-113.
6. Mishra, R 2010, 'MRI based brain tumor detection using wavelet packet feature and artificial neural networks', *Proceedings of the International Conference and Workshop on Emerging Trends in Technology 2010*.
7. Quart-UI-Ain, Ghazanfar Latif, Sidra Batool Kazmi, M, Arfan Jaffer & Anwar M Mirza 2009, 'Classification and Segmentation of Brain Tumor using Texture analysis', *International Journal of Innovative Computing, Information and Control*.
8. Rajendran, P & Madheswaran, M 2009, 'An Improved Image Mining Technique For Brain Tumor Classification Using Efficient classifier', *International Journal of Computer Science and Information Security*, vol. 6, no. 3, pp.107-116.
9. Sasikala, M & Kumaravel, N 2008, 'A wavelet-based optimal texture feature set for classification of brain tumors', *Journal of Medical Engineering and Technology*, vol. 32, no.3, pp. 198-205.
10. Sebe, N & Michael SL 2000, 'Wavelet based texture classification', *proceeding of 15<sup>th</sup> International conference on Pattern Recognition*, pp. 3952-3962.
11. Shufu Xie, Shiguang Shan, XilinChenandJie Chen 2010, 'Fusing Local Patterns of Gabor Magnitude and Phase for Face Recognition', *IEEE Transactions on Image Processing*, vol. 19, no. 5, pp.1349-1362.
12. Wen Zhu, Nancy Zeng & Ning Wang 2010, 'Sensitivity, Specificity, Accuracy, Associated Confidence Interval and ROC Analysis with Practical SAS Implementations', *Proceedings of the SAS Conference, Baltimore, Maryland*.